

Forecasting urban land expansion and heat island intensification globally through 2050

1 Abstract

By 2050, about 6 billion people, nearly 66% of the global population, will live in urban areas¹, where temperature are projected to increase by 2~4°C due to greenhouse gases (GHG) induced global warming². Although this rapid urbanization process is projected to result in urban land expansion by 300% from 2010³, little is known about how the expansion will intensify urban heat island (UHI) effects globally, causing additional warming. Here, we improved and updated the previous spatially explicit forecasts of urban expansion⁴, which is then used in a location-based model to forecast UHI intensification. We show, with higher confidence than previously forecasted, that more medium to large urban areas are emerging, especially in Asia and Africa. In these regions, UHIs will intensify more in smaller urban areas that grow into medium to large ones, particularly in those geographically close to, and thus are affected by advection from, other larger urban areas. Since these currently smaller Asian and African urban areas are usually less capable of adapting to climate change^{2,5}, our forecasts of UHI intensification suggest great challenges for them to develop adaptive capacity, and to coordinate adaptation with nearby municipalities, in such a short time window.

2 Introduction

As greenhouse gases (GHG) continue to build up in the atmosphere changing the climate, numerous studies⁶⁻⁸ have downscaled the effects of global warming to cities, where more than half of the world's population live¹. Such attempts to overlap climate change with cities have shown² that many major urban centers will experience 2~4°C warming by the mid-century. Concomitantly, as global urban population will grow by ~3 billion and urban lands expand by ~300% from 2010³, additional warming on top of GHG-induced climate change is expected, since the urban heat island effects been shown^{9,10} to escalate with the logarithmic sizes of urban areas. However, little is known about how much urbanization-induced warming will vary globally, causing different degrees of warming when combined with GHG-induced climate change. This information is critical for climate adaptation, because adversary consequences from warming, such as mortality/morbidity rates^{11,12} and energy consumption¹³, tend to increase exponentially with temperatures.

Although urban size is the key variable to predicting future UHI intensification, the previous spatially explicit probabilistic forecasts of global urban expansion⁴ fail to replicate the size distribution of the Zipf's law, which describes the linear inverse relationship between ranks and sizes on logarithmic scales. Without considering Zipf's law in the forecasts, we cannot differentiate magnitudes of growth for urban areas with various sizes on a logarithmic scale, and thus fail to reliably predict the size-dependent UHI intensity. In this paper, we add constraints of Zipf's law to a global urban expansion model⁴, in order to maintain the rank-size distribution in our forecasts.

In addition to size, recent studies suggest that the UHI intensity also depends on 1) nearby UHIs^{14,15} (Figure S 6), due to the horizontal advection of warm air; and 2) background climates¹⁶, since contributions to UHI from various factors are climate-dependent. These two factors will become more important in the coming decades, because 1) more mega-urban regions (UHRs), clusters of nearby urban areas, are emerging across the world¹⁷ and 2) future urban expansion is more likely to occur in tropic/sub-tropics rather than in temperate climates as in the history⁴. However, these factors were rarely considered in UHI prediction¹⁸, due to the lack of spatially explicit and size distribution preserved forecasts of urban land expansion, which are now available in the updated forecasts. To utilize this new spatial information in forecasting UHI intensification, we apply the spatial regression to model UHI intensity as a function of size on a logarithmic scale^{9,10} (Figure S 5), nearby UHIs (Figure S 6), and the background climates¹⁶, while controlling other relevant biophysical features, such as surface albedo and vegetation abundance.

3 Methods

Two models are built to forecast UHI intensifications globally: 1) a spatially explicit, probabilistic urban expansion model to predict the likelihood of a location to become urban land, and 2) a spatial resolved UHI model to relate increasing urban sizes with escalating temperature. Applying these two models on the Shared Socioeconomic Pathways (SSPs)¹⁹, we can forecast the future urban land expansion and heat island intensification through 2050 resulting from socioeconomic development across the world.

The urban expansion model is modified from a previous global forecast model, URBANMOD⁴, which first predicts the quantities of urban land then allocates them spatially. We modified both the quantity prediction and land allocation processes to develop a new forecast model, called URBANMOD-ZIPF. Instead of a simple linear regression in URBANMOD, a fixed effect panel data regression is used in URBANMOD-ZIPF, to model urban land per capital (ULC) as a function of GDP per capital (GDPC) and the percentage of urban population (URB). With the 32 regions defined in the SSP database²⁰ as analytical units, to derive ULC, GDPC and URB, we use GDP and population statistics from the World Bank, urbanization rates from the United Nations¹, and urban lands from the Global Human Settlement Layer (GHSL)²¹. A panel data regression is built on historical observations in 1990 and 2000:

$$ULC_{it} = \beta_0 + \beta_1 GDPC_{it} + \beta_2 URB_{it} + \sum_{j=2}^N \gamma_j D_{ij} + \varepsilon_{it} \quad i = 1 \dots N, t = 1990, 2000$$

where β_0 is a constant, β_1 and β_2 are the coefficients of GDPC and URB, γ_j is the coefficient of the regional dummies D_{ij} , ε_{it} is the error term, and N is the number of regions. Applying this equation on the future GDPC²² and URB²³ in SSPs, we can forecast the quantities of urban lands in each scenario through 2050. In URBANMOD, the forecasted urban lands are allocated using a spatially explicit grid-based model²⁴, based on urban development suitability derived from slope, distance to roads, population density, and land cover. Here, in URBANMOD-ZIPF, we modify the allocation process by constraining the Zipf's law distribution of urban sizes. Considering the fact that Zipf's law is maintained because the growth rate of an urban area is proportional to its size²⁵, we multiply the probability of a grid to be urbanized by the size of the adjacent urban area.

The UHI model is based on existing literature that relate UHI intensities with logarithmic urban sizes¹⁰, nearby UHIs^{14,26}, background climates¹⁶ and other biophysical characteristics^{27,28} of the urban area. To take into account the spatial effects of nearby UHIs, a spatial lag model is used:

$$UHI_i = \rho \sum_j^N w_{ij} UHI_j + \beta X_i + \varepsilon_i$$

where vector β contains coefficients for the urban feature vector X_i that contains logarithmic urban size and other biophysical characteristics, such as vegetation abundance, albedo, surface roughness, of the i -th urban area; ρ is the spatial lag coefficient that account for the effects from nearby UHIs weighted by the inverse square distances, $w_{ij} = \sum_j d_{ij}^{-2}$ (d is distance between i and j); and ε_i is the error term. To distinguish different contributions of these factors in different climates, we build this model separately for urban areas in each climate zone: arid, boreal, equatorial and temperate. The extents of urban areas are derived from GHSL. Within urban extents, biophysical characteristics are obtained from various remote sensing products. UHIs are measured by subtracting land surface temperature (LST) within urban extent by that of the buffer zone. LSTs of the urban area and its buffer zone are obtained from the MOD/MYD 11A2 products.

4 Results and Discussions

By adding constraints of the Zipf's law to the previous forecast model (URBANMOD⁴), we update the previous urban land expansion forecasts (URBANMOD-ZIPF), in which the rank-size distribution observed in historical patterns is maintained (Figure S 1). Validations against actual urban lands suggest higher accuracies of the updated forecasts over the previous ones, both on amounts and locations of urban expansion. Figure S 2 shows that the previous forecasts have underestimated the amount of urban expansion, especially for regions with more than 200 km urban land per million persons, which are corrected in the updated forecasts. In terms of locations, as shown in validations of forecasted urbanization against actual urban lands expansion from 2000 to 2015, the updated forecasts improve accuracy by 72% over the previous ones (Table S 1), especially for medium to large urban areas, whose sizes are greater than 100 km² (Figure 1-A). Compared to the previous forecasts through 2030, our analysis shows, with higher confidence, that more urban land expansion will likely to occur near existing medium to large urban areas (Figure 1-B). The underestimation of previous forecasts is more prominent near larger urban areas in China, India, Indonesia, and Sub-Saharan African countries (Figure S 3). Extending the updated forecasts to 2050 under different shared socioeconomic pathways (SSPs), our analysis shows that, compared to elsewhere, more urban land expansion will occur in Africa (MAF) and Asia (ASIA), as shown in Figure 2. In these two regions, across all scenarios (Figure S 4), the amounts of expansion near existing urban areas of all sizes will be as nearly twice as their counterparts in other regions. Considering the current lack of economic and political power for climate adaptation in these regions⁵, the potential warming resulting from this rapid urban expansion presents substantial challenges for building adaptive capacity in the narrow time window of just a few decades.

Compared to the non-spatial model that neglects the nearby UHIs and background climates, the spatial model achieve better agreement with observations, especially for daytime UHI (Table S 2). Applying the spatial UHI model to the forecasted urban land expansion, we generate the forecasts of UHI intensification globally from 2015 to 2050 (Figure 3 and Figure 4-B). As can be seen from Figure 3, UHI intensity will increase more strongly in urban areas with more urban

land expansion. The intensification is even stronger for smaller urban areas that grow into medium to larger ones, as shown in the upper left of Figure 3, because their sizes increase more logarithmically compared to already large urban areas that grow larger. These small- or medium-to-large urban expansions and the resulting stronger heat island intensification, as shown in Figure 4-B, will mostly occur in Eastern Europe (REF) and Africa (MAF). Most of these smaller urban areas²⁹, especially those in Africa⁵, currently lack the economic and political resources to adapt. The forecasted rapid warming suggests urgent yet challenging needs for these urban areas to build up adaptive capacity in such a narrow time window. As shown in Figure 3, UHI intensify more strongly in the *core* urban areas (circle), which are the largest within a radius of 50 km, than in the *peripheral* ones, which are smaller than nearby ones, even with the comparable amounts of expansion. The extra warming in *peripheral* urban areas results from the spatial advection of warm air, because they are closer to other urban areas with stronger UHIs. Figure 4-B shows that this trend of stronger warming in *peripheral* urban areas is more likely to occur in Eastern Europe, Africa, and Asia. To mitigate the warming from nearby UHIs, a *peripheral* municipal government have to implement mitigation measures not just inside its boundary but also in nearby municipalities, which can be a daunting challenge. Our analyses support the emerging argument for the needs of regional, coordinative, multi-scale urban climate adaptation planning³⁰, particularly for urban areas in less developed regions.

This analysis has one caveat worth discussing. The forecasts assume that all future urban lands in each region have the same population density predicted by the corresponding socioeconomic scenario. Yet, this characteristic of urban forms can be altered by planning policies³¹ such as zoning, growth boundary, and public-transport subsidy. Altering population densities changes the surface roughness, the shape of urban canyon and the anthropogenic heat flux, all of which can affect urban temperature by modifying the surface energy balance^{16,32}. Moreover, other urbanization forecasts^{33,34}, although not spatially explicit, have shown that higher densities can reduce urban energy use for transportation and maintaining indoor thermal comfort. Reducing total energy use can mitigate the additional warming effects from GHG, while lowering energy required for indoor cooling can alleviate the burdens of energy systems during high temperatures to avoid catastrophic blackouts³⁵. Further studies are still needed to explore the co-benefits and trade-offs of altering urban population densities in terms of mitigating both urbanization- and GHG-induced warmings. These studies are especially imperative for less developed regions, such as Asia, Eastern Europe, and Africa, where, as our forecasts show, large areas of urban lands are yet to be built and thus density alteration is relatively easier.

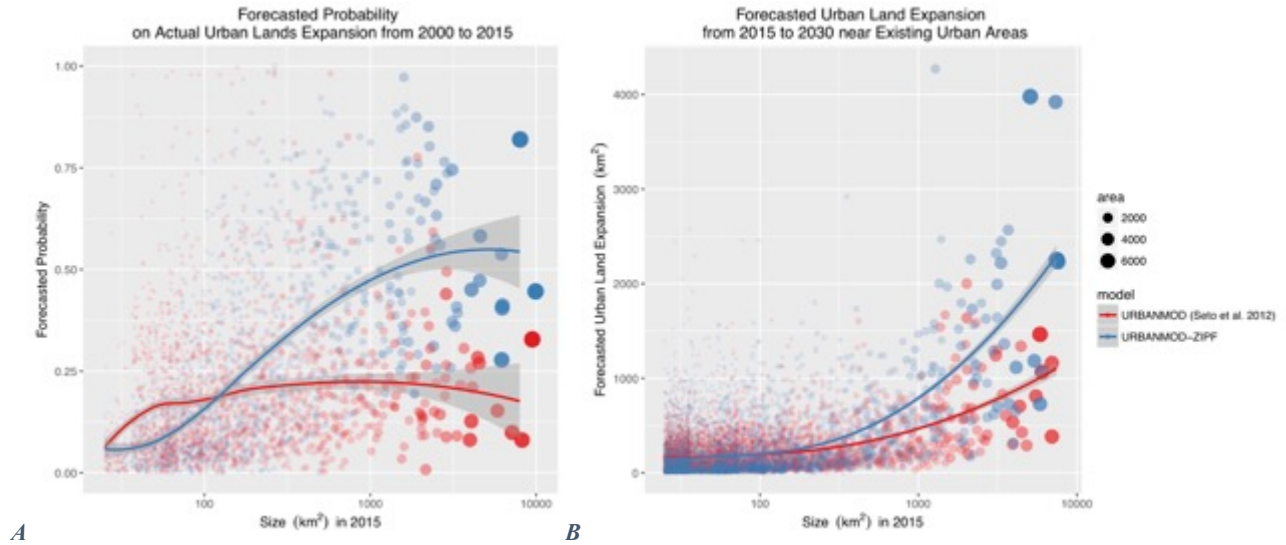


Figure 1 Comparison of the previous and the updated urban land expansion forecasts. a) Probability of urbanization predicted by URBANMOD and URBANMOD-ZIPF on the new urban lands from 2000 to 2015 with various sizes (km^2). b) Urban land expansion from 2015 to 2030, within 50 km of existing urban areas in 2015, forecasted by URBANMOD⁴ and URBANMOD-ZIPF. Horizontal axes on log scale.



Figure 2 Urban land expansion from 2015 to 2050 under SSP5 scenario forecasted by URBANMOD-ZIPF. Vertical axis represents the forecasted amount of new urban lands within a radius of 50 km around existing urban areas in 2015; horizontal axis represents the sizes of urban areas in 2015. Different colors represent urban areas in five different regions.

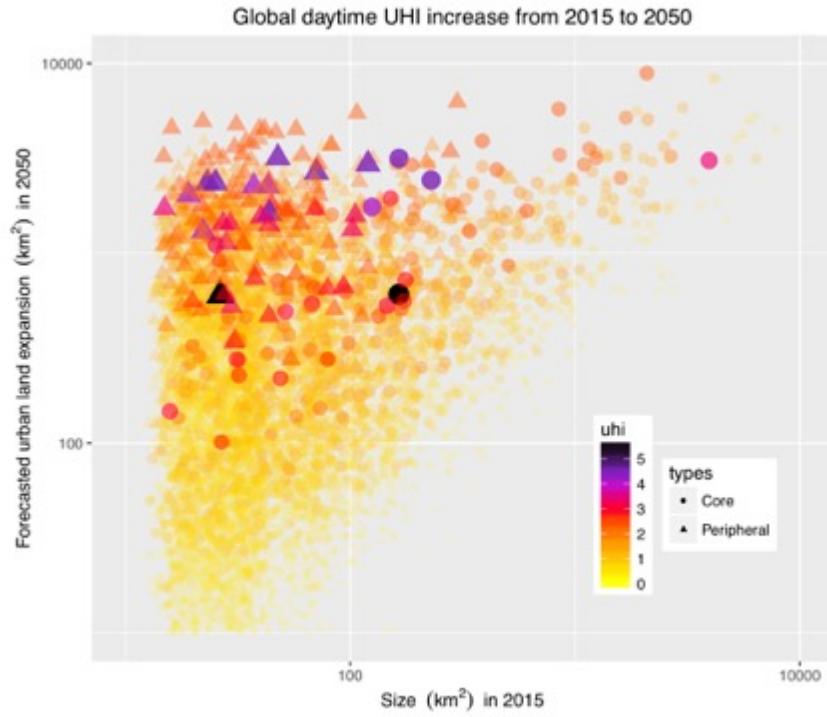


Figure 3 Global daytime UHI increase from 2015 to 2050, in urban areas with different sizes and magnitudes of expansion. Same as in Figure 2, horizontal and vertical axes show the size of urban area in 2015 and the forecasted urban land expansion within a radius of 50 km. Circles represent core urban areas, which are larger in size than other urban areas within 50 km; while triangles represent peripheral urban areas, which are smaller than others within 50 km. Colors indicate different magnitudes of increases of UHI intensity (•).

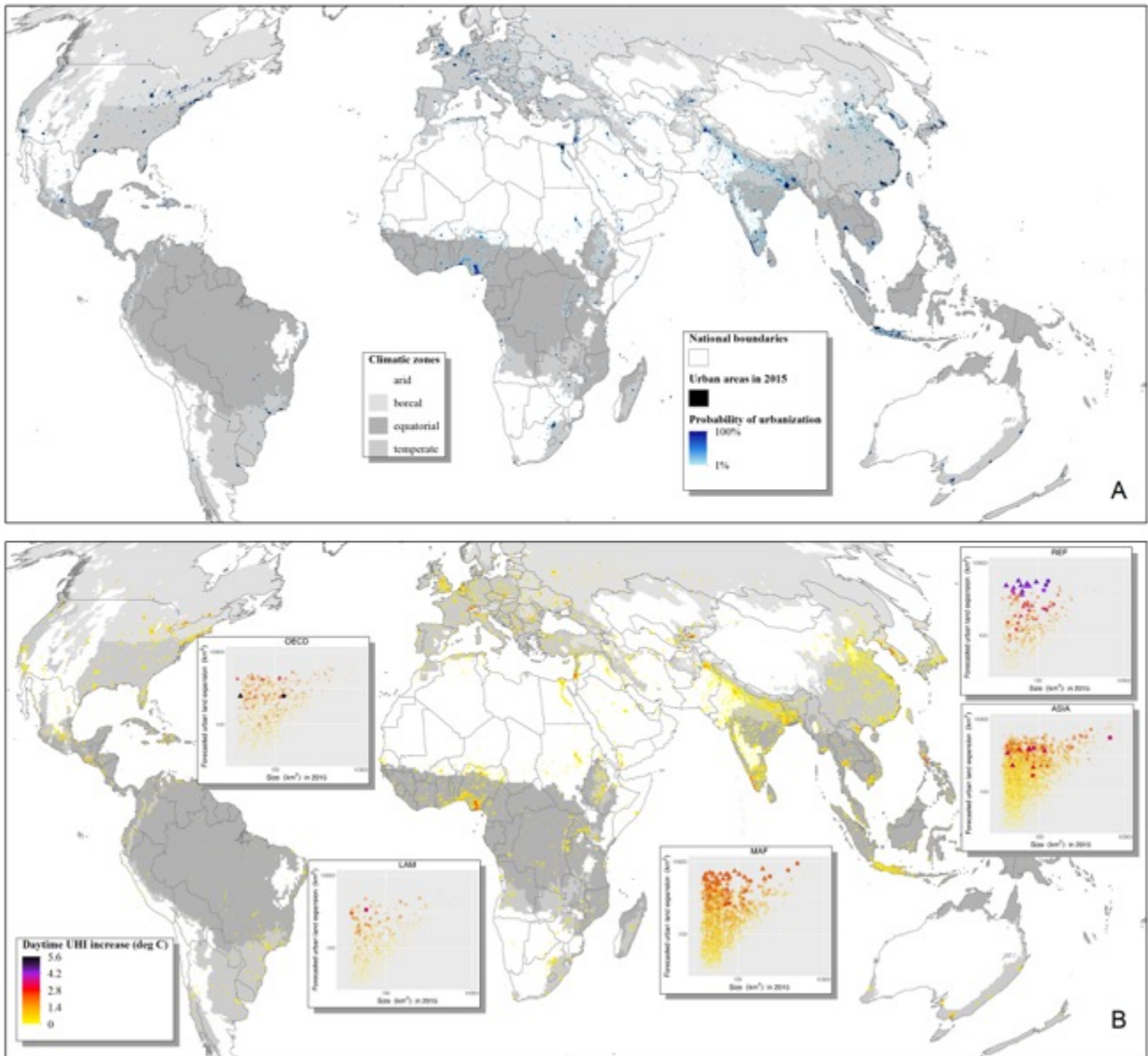


Figure 4 Global forecasts of (A) probabilities of urban expansion and (B) the expected increase of daytime UHI (temperature times probability) from 2015 to 2050 under SSP5 scenario. Subplots in (B) are the same as Figure 3, except that each subplot represents one region of the world.

5 References

1. UN DESA. *World Urbanization Prospects: The 2014 Revision, Highlights*. (United Nations, Department of Economic and Social Affairs, Population Division, 2014).
2. Revi, A. *et al.* Urban areas. in *Climate Change 2014: Impacts, Adaptation, and Vulnerability. Part A: Global and Sectoral Aspects. Contribution of Working Group II to the Fifth*

- Assessment Report of the Intergovernmental Panel of Climate Change* (eds. Field, C. B. et al.) 535–612 (Cambridge University Press, 2014).
3. Angel, S., Parent, J., Civco, D. L., Blei, A. & Potere, D. The dimensions of global urban expansion: Estimates and projections for all countries, 2000–2050. *Prog. Plan.* **75**, 53–107 (2011).
 4. Seto, K. C., Güneralp, B. & Hutya, L. R. Global forecasts of urban expansion to 2030 and direct impacts on biodiversity and carbon pools. *Proc. Natl. Acad. Sci.* **109**, 16083–16088 (2012).
 5. Carmin, J., Nadkarni, N. & Rhie, C. Progress and challenges in urban climate adaptation planning: results of a global survey. *Camb. MA Mass. Inst. Technol.* (2012).
 6. Rosenzweig, C. *et al.* Mitigating New York City’s Heat Island: Integrating Stakeholder Perspectives and Scientific Evaluation. *Bull. Am. Meteorol. Soc.* **90**, 1297–1312 (2009).
 7. Wilby, R. . A Review of Climate Change Impacts on the Built Environment. *Built Environ.* **33**, 31–45 (2007).
 8. Adachi, S. A., Kimura, F., Kusaka, H., Inoue, T. & Ueda, H. Comparison of the Impact of Global Climate Changes and Urbanization on Summertime Future Climate in the Tokyo Metropolitan Area. *J. Appl. Meteorol. Climatol.* **51**, 1441–1454 (2012).
 9. Oke, T. R. City size and the urban heat island. *Atmospheric Environ.* **1967** **7**, 769–779 (1973).
 10. Zhou, B., Rybski, D. & Kropp, J. P. On the statistics of urban heat island intensity. *Geophys. Res. Lett.* **40**, 5486–5491 (2013).
 11. Gasparrini, A. *et al.* Mortality risk attributable to high and low ambient temperature: a multicountry observational study. *The Lancet* **386**, 369–375 (2015).

12. McGeehin, M. A. & Mirabelli, M. The potential impacts of climate variability and change on temperature-related morbidity and mortality in the United States. *Environ. Health Perspect.* **109**, 185–189 (2001).
13. Zhao, H. & Magoulès, F. A review on the prediction of building energy consumption. *Renew. Sustain. Energy Rev.* **16**, 3586–3592 (2012).
14. Zhang, D.-L., Shou, Y.-X. & Dickerson, R. R. Upstream urbanization exacerbates urban heat island effects. *Geophys. Res. Lett.* **36**, L24401 (2009).
15. Zhang, D.-L., Shou, Y.-X., Dickerson, R. R. & Chen, F. Impact of Upstream Urbanization on the Urban Heat Island Effects along the Washington–Baltimore Corridor. *J. Appl. Meteorol. Climatol.* **50**, 2012–2029 (2011).
16. Zhao, L., Lee, X., Smith, R. B. & Oleson, K. Strong contributions of local background climate to urban heat islands. *Nature* **511**, 216–219 (2014).
17. Seto, K. C., Golden, J. S., Alberti, M. & Turner, B. L. Sustainability in an urbanizing planet. *Proc. Natl. Acad. Sci.* **114**, 8935–8938 (2017).
18. Estrada, F., Botzen, W. J. W. & Tol, R. S. J. A global economic assessment of city policies to reduce climate change impacts. *Nat. Clim. Change* **7**, 403 (2017).
19. O’Neill, B. C. *et al.* A new scenario framework for climate change research: the concept of shared socioeconomic pathways. *Clim. Change* **122**, 387–400 (2013).
20. IIASA. *IIASA Shared Socioeconomic Pathways (SSP) database.* (2013).
21. Pesaresi, M. *et al.* A Global Human Settlement Layer From Optical HR/VHR RS Data: Concept and First Results. *IEEE J. Sel. Top. Appl. Earth Obs. Remote Sens.* **6**, 2102–2131 (2013).

22. Crespo Cuaresma, J. Income projections for climate change research: A framework based on human capital dynamics. *Glob. Environ. Change* **42**, 226–236 (2017).
23. Jiang, L. & O’Neill, B. C. Global urbanization projections for the Shared Socioeconomic Pathways. *Glob. Environ. Change* (2015). doi:10.1016/j.gloenvcha.2015.03.008
24. Pontius, R. G., Cornell, J. D. & Hall, C. A. S. Modeling the spatial pattern of land-use change with GEOMOD2: application and validation for Costa Rica. *Agric. Ecosyst. Environ.* **85**, 191–203 (2001).
25. Rozenfeld, H. D. *et al.* Laws of population growth. *Proc. Natl. Acad. Sci.* **105**, 18702–18707 (2008).
26. Zhou, D., Zhao, S., Zhang, L., Sun, G. & Liu, Y. The footprint of urban heat island effect in China. *Sci. Rep.* **5**, 11160 (2015).
27. Peng, S. *et al.* Surface Urban Heat Island Across 419 Global Big Cities. *Environ. Sci. Technol.* **46**, 696–703 (2012).
28. Clinton, N. & Gong, P. MODIS detected surface urban heat islands and sinks: Global locations and controls. *Remote Sens. Environ.* **134**, 294–304 (2013).
29. Aromar Revi *et al.* Towards transformative adaptation in cities: the IPCC’s Fifth Assessment. *Environ. Urban.* **26**, 11–28 (2014).
30. Shi, L. *et al.* Roadmap towards justice in urban climate adaptation research. *Nat. Clim. Change Lond.* **6**, 131–137 (2016).
31. Vigiúé, V. & Hallegatte, S. Trade-offs and synergies in urban climate policies. *Nat. Clim. Change* **2**, 334–337 (2012).
32. Oke, T. R. The energetic basis of the urban heat island. *Q. J. R. Meteorol. Soc.* **108**, 1–24 (1982).

33. Güneralp, B. *et al.* Global scenarios of urban density and its impacts on building energy use through 2050. *Proc. Natl. Acad. Sci.* **114**, 8945–8950 (2017).
34. Creutzig, F., Baiocchi, G., Bierkandt, R., Pichler, P.-P. & Seto, K. C. Global typology of urban energy use and potentials for an urbanization mitigation wedge. *Proc. Natl. Acad. Sci.* **112**, 6283–6288 (2015).
35. Anderson, G. B. & Bell, M. L. Lights out: Impact of the August 2003 power outage on mortality in New York, NY. *Epidemiol. Camb. Mass* **23**, 189–193 (2012).

6 Appendix

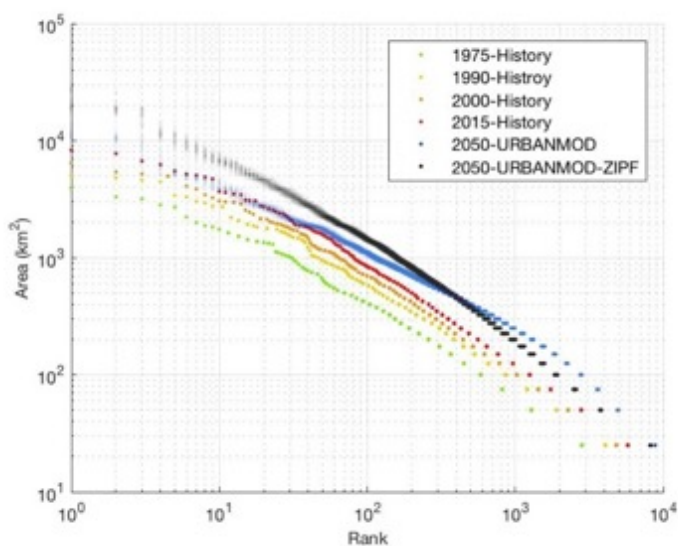
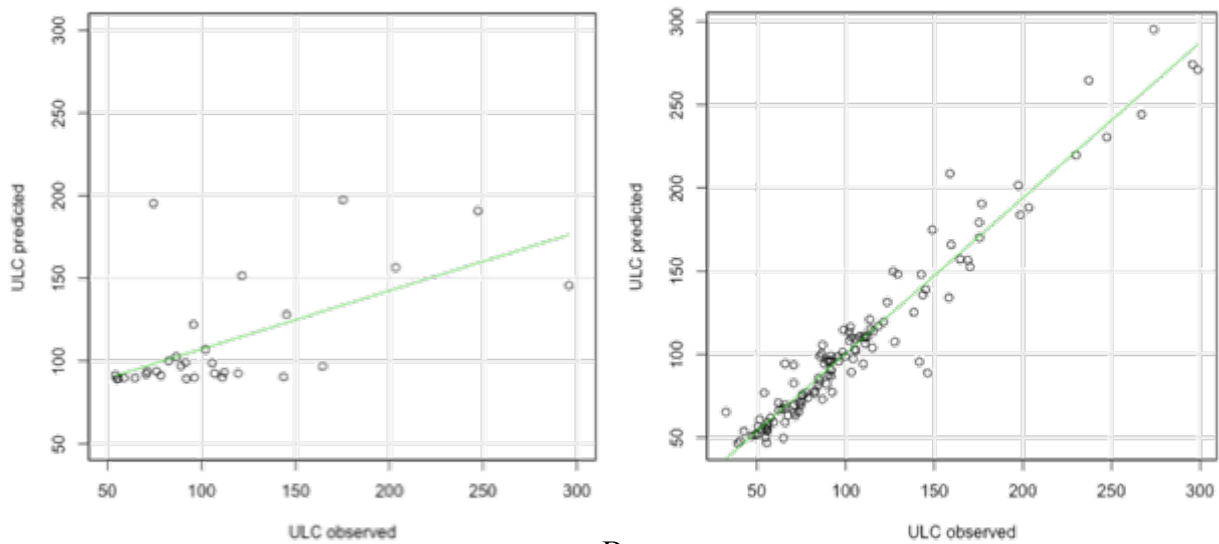


Figure S 1 Rank-Size distributions of historical areas in 1975, 1990, 2000, and 2015, and those in 2050 under SSP5 scenario, forecasted by URBANMOD and URBANMOD-ZIPF. Both ranks and sizes are on log scale.



A **B**
 Figure S 2 Observed versus predicted urban land per capita (ULC) in km² per million persons of 32 regions defined in SSP database. A) Predicted by linear regression on ULC in 2000. B) Predicted by panel data regression on ULC in 1990 and 2000.

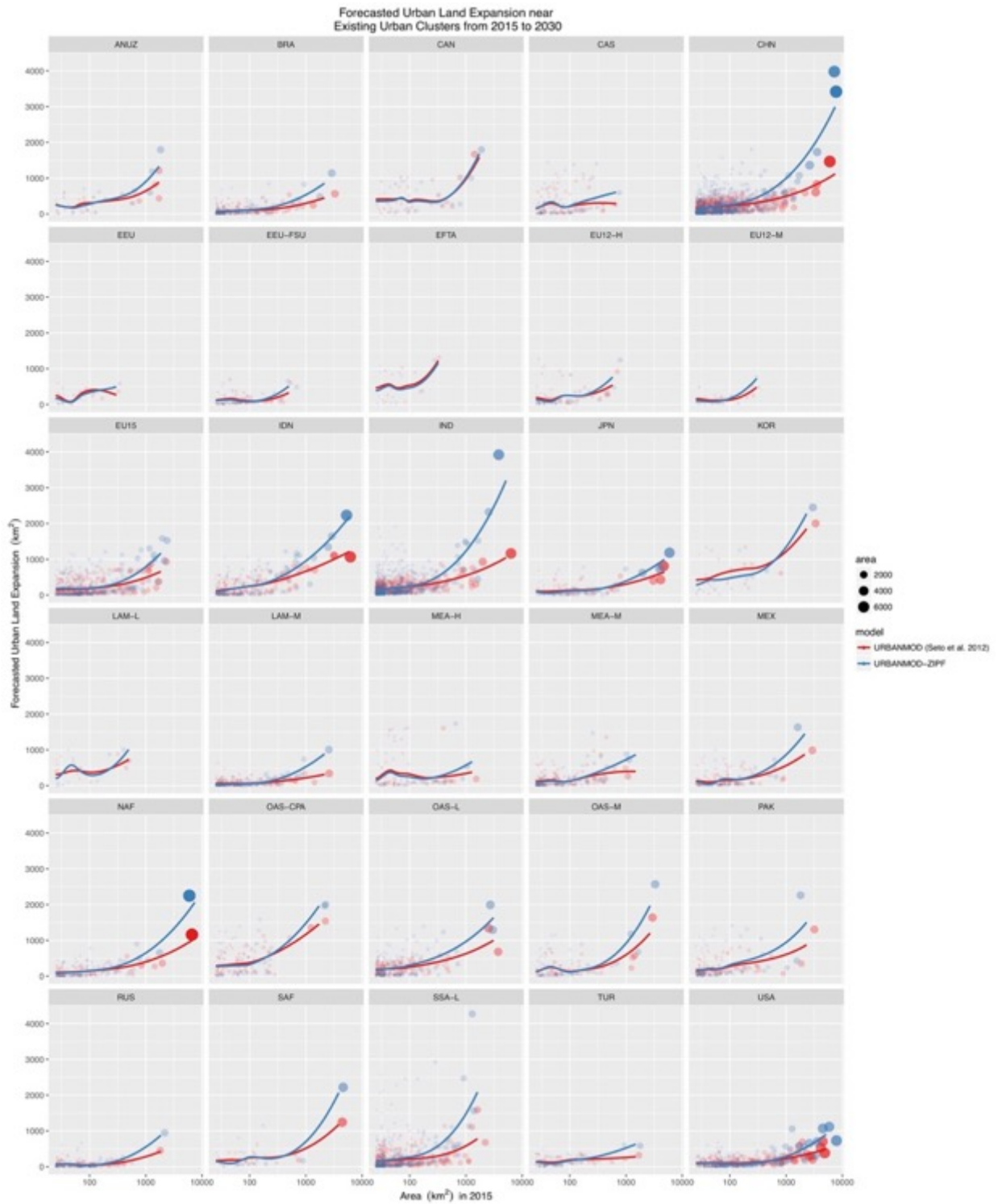


Figure S 3 Expected urban land expansion from 2015 to 2030 in 30 regions, within 50 km of existing urban lands in 2015, forecasted by URBANMOD⁴ and URBANMOD-ZIPF (this work). Horizontal axes are on log scale.

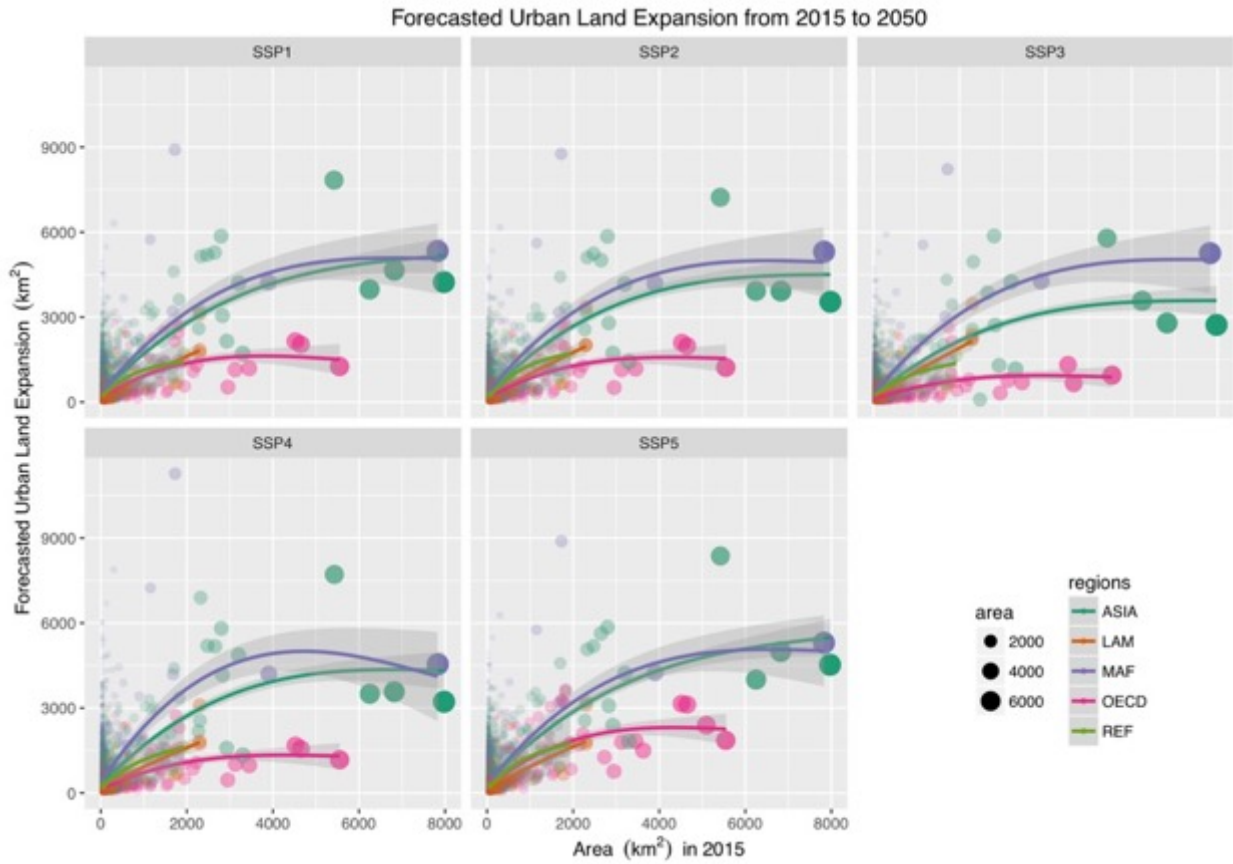
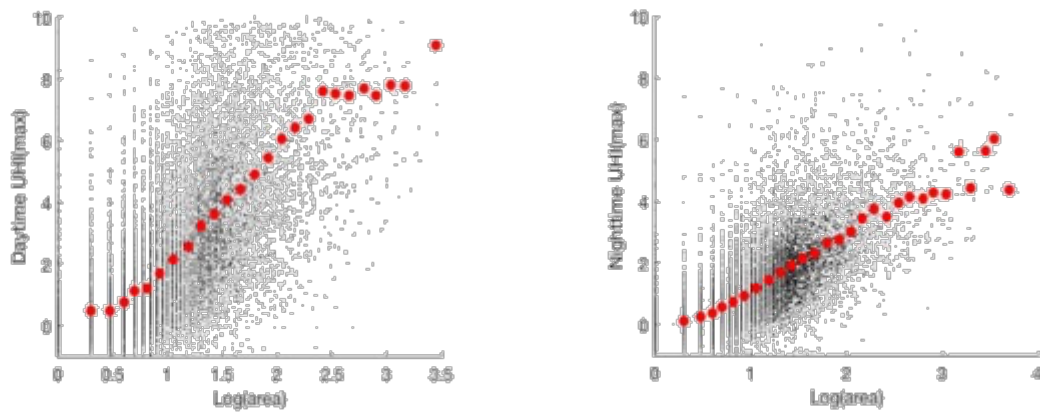


Figure S 4 Urban land expansion from 2015 to 2050 under five SSP scenarios forecasted by URBANMOD-ZIPF. Vertical axis represents the forecasted amount of new urban lands within a radius of 50 km around existing urban clusters in 2015; horizontal axis represents the area of urban clusters in 2015. Colors represent urban clusters in five different regions.



A B
Figure S 5 Daytime (A) and nighttime (B) UHI intensities versus the sizes of urban areas on a logarithmic scale in black dots. Red dots are the bin-average.

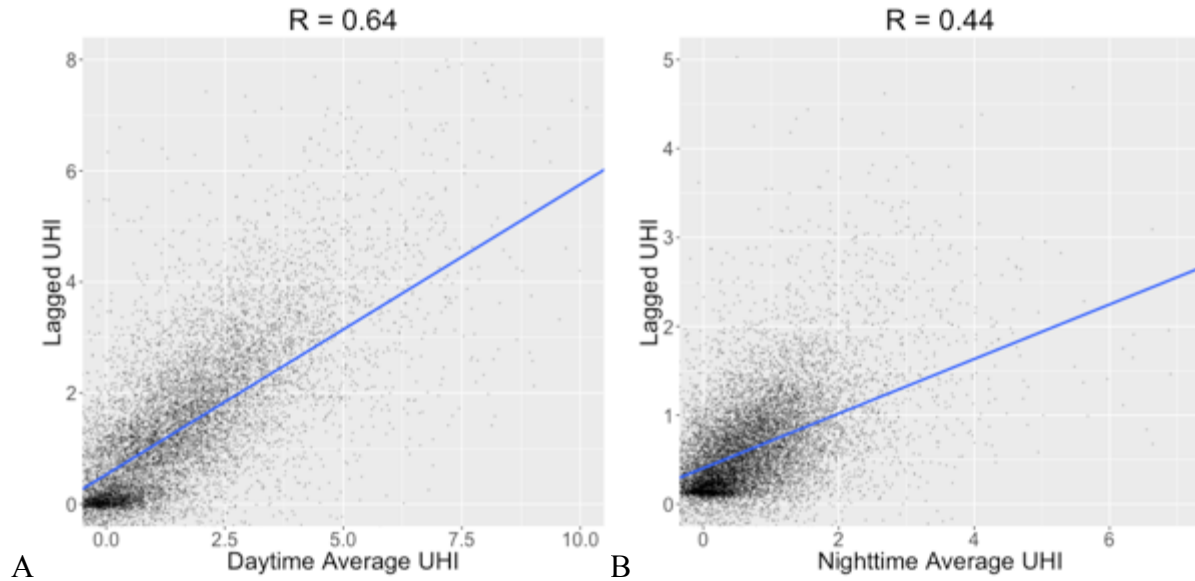


Figure S 6 Daytime (A) and nighttime (B) UHI intensities versus their corresponding spatially lagged values.

Table S 1 Probabilities of becoming urban, forecasted by URBANMOD and URBANMOD-ZIPF, averaged over the locations that were urbanized from 2000 to 2015. The same statistics were also calculated in different climate zones.

Model	Climate				
	All	Arid	Boreal	Equatorial	Temperate
URBANMOD	0.18	0.21	0.21	0.18	0.17
URBANMOD-ZIPF	0.31	0.35	0.32	0.28	0.32

Table S 2 Performance and key coefficients of non-spatial and spatial models for daytime and nighttime UHI.

UHI	Model	r ²	R	RMSE	Climate	Coefficients		
						ρ	Log(Area)	LM-lag
Daytime	None-spatial	0.58	0.76	2.11	All	-	2.06***	-
	Spatial	0.70	0.84	1.51	Arid	0.30***	1.68***	260***
					Boreal	0.12***	3.80***	28***
					Equatorial	0.29***	2.08***	487***
					Temperate	0.31***	2.10***	610***
Nighttime	None-spatial	0.75	0.86	1.02	All	-	1.25***	-
	Spatial	0.76	0.87	0.87	Arid	0.09***	1.28***	38***
					Boreal	0.12***	1.93***	24***
					Equatorial	0.03***	0.83***	5***
					Temperate	0.10***	0.94***	91***

P ≤ 0.05*, P ≤ 0.01**, P ≤ 0.001***